IOPscience iopscience.iop.org

Home Search Collections Journals About Contact us My IOPscience

An X-ray photoemission study of Ce-Rh, Ce-Pd and Ce-Ag interfaces

This article has been downloaded from IOPscience. Please scroll down to see the full text article.

1992 J. Phys.: Condens. Matter 4 8021

(http://iopscience.iop.org/0953-8984/4/40/014)

View the table of contents for this issue, or go to the journal homepage for more

Download details:
IP Address: 171.66.16.96
The article was downloaded on 11/05/2010 at 00:39

Please note that terms and conditions apply.

J. Phys.: Condens. Matter 4 (1992) 8021–8028. Printed in the UK

An x-ray photoemission study of Ce–Rh, Ce–Pd and Ce–Ag interfaces

C Berg and S Raaen

Institutt for Fysikk, Norges Tekniske Høgskole, Universitetet i Trondheim, N-7034 Trondheim, Norway

Received 20 July 1992

Abstract. X-ray photoelectron spectroscopy (XPS) has been employed to study electronic states in Ce–Rh, Ce–Pd, and Ce–Ag interfaces. Thin Ce films were deposited onto evaporated substrates of Rh, Pd and Ag, and conversely, thin films of Rh, Pd and Ag were deposited onto evaporated Ce films. Tetravalent Ce emission was observed in the Rh and Pd systems. Substrate core level attenuation curves show a deviation from exponential decay as material is deposited. Substrate core level shifts as well as the appearance of a tetravalent Ce signal are indicative of interface alloy formation; however, clustering of the evaporated species may also take place.

1. Introduction

Lanthanide-based materials are widely studied due to the rich variety of physical properties which are exhibited in many of these systems. Several rare earth materials are also used in industrial applications, e.g. in electronic materials and in permanent magnets. In this paper, we present a photoemission study of interfaces between cerium and the 4d transition metals rhodium and palladium, as well as silver. Intermetallic compounds based on these materials has been extensively investigated due to the occurrence of 4f valence instabilities in several systems [1–3]. In particular, the system $Ce(Pd_{1-x}T_x)_3$, where T = Rh or Ag, has been shown to span the entire mixed-valence region for Ce, i.e. possessing from $\sim$ 3.2 to 3 valence electrons, depending on the element T and the parameter x [2, 4]. The sensitivity to the chemical environment of the Ce valence state, coupled with the very distinct Ce 3d photoemission from sites of different 4f count, make core level photoemission a powerful technique to study interfaces in systems based on the present elements.

Previous work has shown that mixed interface alloys may form when a rare earth element is deposited onto a metallic substrate at ambient temperatures [5, 6]. The tendency to form mixed alloys is driven by a large negative heat of mixing in the alloy [5], and is thought to be related to anomalous diffusion properties that various metallic elements possess in rare earth matrices [7]. These interfacial alloys are expected to be amorphous in nature, since they form at temperatures well below those where nucleation and crystalline growth normally occur. The presence of vacancies and lattice imperfections will enhance the rate of interdiffusion [8]. This is likely to be particularly important in the case of evaporated substrates, which have been used in this study.

0953-8984/92/408021+08$07.50 © 1992 IOP Publishing Ltd

Several growth modes of an interface must be considered. In addition to mixed interface alloy formation, several modes of overlayer growth may occur: (i) Frank–van der Merwe, being monolayer by monolayer growth, (ii) Stranski–Krastanov, being the formation of one or two layers followed by clustering, and (iii) Volmer–Weber where the adatoms start clustering immediately [9]. By monitoring substrate core level intensities as material is deposited, it is possible to distinguish between even overlayer growth on the one hand, and clustering or alloy formation on the other hand. Various models of clustering and alloying may give similar substrate core level intensity attenuation profiles, so the possible presence of a tendency to form interfacial alloys must be deduced from an analysis of core level shifts.

The present work was motivated by recent observations of the growth of mixed interfacial alloys following deposition of rare earth elements onto various metallic substrates at ambient temperatures [6], and seeks to describe the electronic structure and morphology of the Ce–Rh, Ce–Pd, and Ce–Ag interface systems by the use of x-ray photoelectron spectroscopy (XPS).

2. Experimental details

The XPS spectra were recorded using a HA-50 hemispherical electron energy analyser from Vacuum Science Workshop (VSW) in conjunction with a twin-anode x-ray source (VSW). An instrumental resolution of about 1 eV was obtained. The samples were prepared *in situ* by evaporating the metals onto a Ta foil, using resistively heated tungsten baskets which were initially thoroughly outgassed. A liquid nitrogen cryostat was in thermal contact with the Ta foil, allowing the samples to be cooled to about 100 K. The foil was cleaned by passing a large current through it, heating it to $> 2000\,^{\circ}C$. In the same way the samples could be carefully heated. The evaporation rates were estimated from evaporation on clean Ta, which is considered to be a non-interacting substrate. The area of the substrate core level peak was measured after subtraction of a Shirley-type background. Both spin–orbit-split components were included in the estimates of the metal 3d emission intensities. Deposition rates were estimated from the measured attenuation of substrate core level intensities. As substrates, films of > 100 Å were evaporated to mimic thick samples. A careful calibration of the evaporation rates was performed, before and after each measurement series, to verify that the evaporation rates were constant. The base pressure in the chamber was about 2×10^{-10} Torr. Oxidation was performed at a pressure of 1×10^{-7} Torr, except for in heavy exposures which were done at 1×10^{-6} Torr. The oxygen 1s (Augér O(KVV) for the palladium samples) level in the chamber was monitored during all experiments.

3. Results

We have studied the interface formation between the rare earth metal cerium and the 4d transition metals rhodium and palladium and the noble metal silver. These systems have been investigated both with cerium overlayers on metal substrates, and vice versa, cerium substrates and metal overlayers.

3.1. The Ce–Pd system

Ce was evaporated onto a > 100 Å thick Pd substrate at an evaporation rate of (2.0 ± 0.3) Å min^{-1}. Conversely, ~ 100 Å Ce was put down as a substrate, onto which a Pd overlayer was evaporated. The Pd evaporation rate was estimated to be (0.8 ± 0.3) Å min^{-1}. When Ce was evaporated onto the Ta foil, a thinner overlayer than expected from the Ce evaporation rate was measured. As no shifts were observed in Ta or in Ce, we assume that Ce has formed small islands or clusters on top of one or two monolayers on the Ta surface (Stranski–Krastanov growth), and that no intermixing has taken place. No clustering was observed when Pd was put down onto the Ta foil to form a substrate film.

The substrate core level intensity was monitored as the overlayer material was evaporated. The relative attenuations of the core level intensities are plotted as functions of the overlayer evaporation time in figure 1. Figure 1(*a*) shows the attenuation of Pd 3d as Ce is deposited whilst (*b*) shows the Ce 3d attenuation as Pd is deposited. The solid curve in both figures represents the exponential attenuation which would be expected for the evaporation of an even overlayer on a non-interacting substrate. For both systems the data points show less attenuation than the ideal exponential decay, indicating that a non-homogeneous overlayer has been formed.

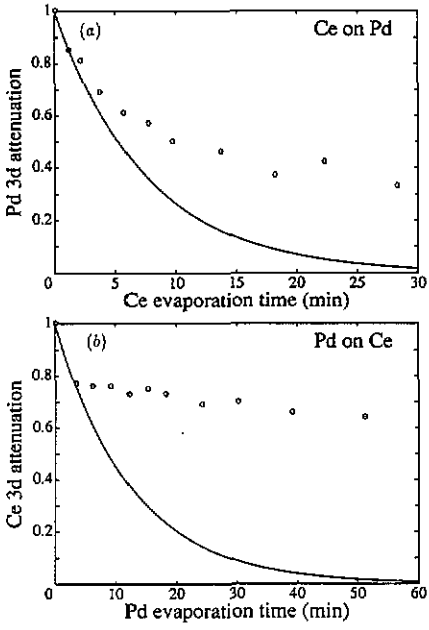

Figure 1. (*a*) Attenuation of Pd 3d photoemission as Ce is deposited at a rate of ~ 2 Å min^{-1}. (*b*) Attenuation of substrate Ce 3d emission with deposition of a Pd overlayer at a rate of ~ 0.8 Å min^{-1}. The solid curve shows exponential decay, as would be expected from the formation of a homogeneous overlayer.

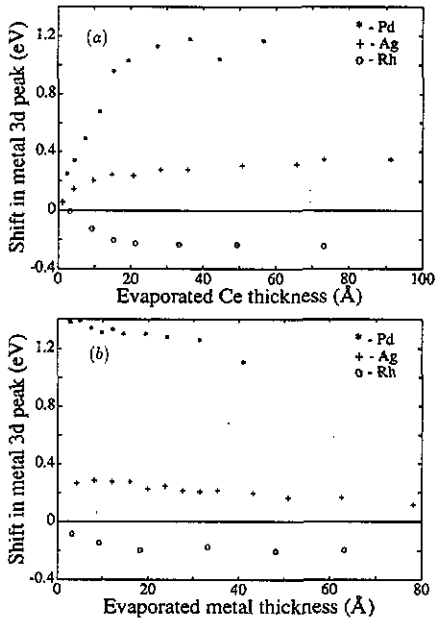

Figure 2. (*a*) Shifts in the position of the transition metal $3d_{5/2}$ peak (○, Rh; ∗, Pd; +, Ag) as Ce is deposited on the metal substrate. The film thicknesses have been calculated from the respective estimated evaporation rates. Note that the positive axis represents shifts to higher binding energies, measured relative to a thick film substrate. (*b*) Metal $3d_{5/2}$ shifts as the metal (○, Rh; ∗, Pd; +, Ag) is deposited on a Ce substrate.

Large core level shifts are observed in Pd in both systems. For the Ce on Pd system the shifts are shown in figure 2(*a*). All shifts are measured relative to the corresponding core level peak position in a thick film. The Pd $3d_{5/2}$ peak position shifts to higher binding energies (E_B) as Ce is evaporated, reaching a value of 1.1 eV when the overlayer is ~ 30 Å thick. When Pd is evaporated on Ce, an initial shift of 1.4 eV to higher E_B is observed in Pd. The shift decreases again as the Pd layer gets thicker, as shown in figure 2(*b*). The precise magnitudes of the Ce shifts are harder to measure, as the Ce 3d peaks are much broader and more complicated than the Pd 3d peaks due to the presence of multiplet splitting and three spin–orbit multiplets, but generally they are found to be of similar magnitudes to the transition metal shifts, and always tend toward higher binding energies.

Figure 3 shows the Ce 3d spectra for samples where Ce is evaporated on Pd. Pure cerium metal shows only trivalent photoemission—the Ce $4f^1$ spin–orbit doublet peaks as indicated in figure 3. The appearance of a $4f^0$ Ce signal is evidence of the formation of Ce–Pd compounds or alloys. For simplicity we will refer to this signal as tetravalent Ce emission, although Ce does not actually possess an integer 4+ valence state [10]. Tetravalent as well as trivalent Ce emission could be recognized from the Ce 3d spectrum, shown in the lower curve of figure 3, for ~ 4 Å Ce on Pd. The Ce $4f^2$ peaks are due to a final-state effect in the photoemission process [11]. When the thickness of the cerium overlayer exceeds ~ 15 Å, only trivalent cerium is observed (middle curve, figure 3). Upon heating a sample with a 15 Å Ce overlayer, which initially showed only trivalent Ce emission, a strong Ce $4f^0$ peak emerged, as shown in the upper curve of figure 3. Cooling of a system similar to the one in the lower graph (~ 4 Å Ce on Pd) showed no detectable change in the Ce $4f^0$ signal intensity. When Pd was evaporated on a Ce substrate, no tetravalent Ce was observed at any Pd overlayer thickness.

To investigate further the nature of the overlayer system that showed both trivalent and tetravalent Ce emission (~ 4 Å Ce on Pd), the system was oxidized stepwise up to 500 L (1 Langmuir=exposure of 1×10^{-6} Torr s^{-1}). The development of the Ce 3d spectrum is shown in figure 4. The intensity of the Ce $4f^0$ peak increases with oxygen exposure, and a shift to higher binding energies is seen, increasing to 2.2 eV after ~ 100 L. After 500 L we still observe some of the Ce $4f^1$ signal, i.e. not all the Ce_2O_3 has been converted to CeO_2 [12]. By comparison to tetravalent Ce in CeO_2 [12], one sees from the shape of the peaks that the initial tetravalent signal arises from metallic cerium, as confirmed by the absence of oxygen emission.

3.2. The Ce–Rh system

Figure 5(*a*) shows the relative Rh 3d intensities as Ce was evaporated onto a ~ 180 Å thick Rh film at a rate of (2.2 ± 0.5) Å min^{-1}. Figure 5(*b*) shows the substrate core level attenuation for the inverse system, a Ce substrate with an Rh overlayer. Rh was evaporated at a rate of (2.7 ± 0.5) Å min^{-1}. Again the attenuation is less than the exponential decay of an even overlayer growth. When Ce was evaporated on Rh we measured a shift in the Rh $3d_{5/2}$ peak to lower binding energies, increasing in size with increasing Ce coverage, measuring -0.2 eV after evaporation of ~ 20 Å Ce (figure 2(*a*)). For the Rh on Ce system, the shift of the Rh $3d_{5/2}$ peak was again to lower binding energies, about -0.2 eV in a ~ 20 Å thick Rh film. For the Ce on Rh system the Ce 3d spectra (figure 6) show that Ce has reacted to form an interface alloy, as both tetravalent and trivalent Ce photoemission are observed. The presence

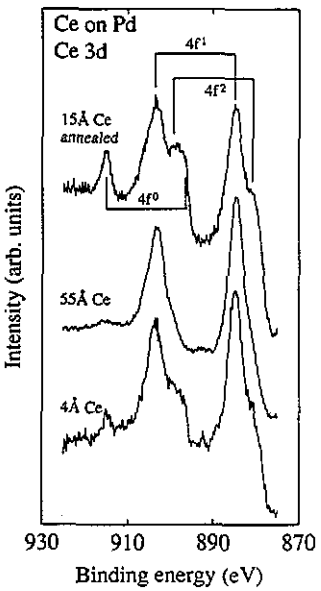

Figure 3. Ce 3d core level positions after a deposition of ~ 4 Å Ce on a Pd substrate (lower graph), ~ 55 Å Ce on Pd (middle graph) and after heating a sample with ~ 15 Å Ce on Pd (upper graph).

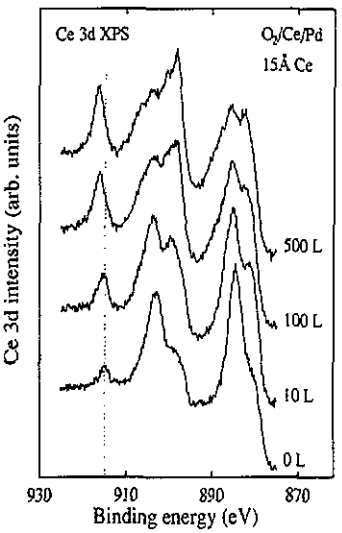

Figure 4. Ce 3d core level spectra of a sample with ~ 15 Å Ce on Pd, before and during oxidation up to 500 L oxygen exposure. Notice the growth and the shift of the $4f^0$ peak which was initially at 915 eV binding energy.

of oxygen at about the 3% level is believed not to be the cause of the $4f^0$ emission in the Ce 3d spectra. The Ce $4f^0$ signal is strongest when the Ce overlayer thickness is ~ 15 Å, but is still present in an overlayer of ~ 75 Å thickness. When Rh was evaporated on Ce no tetravalent Ce signal was observed initially. But in overlayers thicker than ~ 70 Å both Ce $4f^1$ and Ce $4f^0$ emissions were seen.

3.3. The Ce–Ag system

The Ce–Ag system, as for the previous systems, has been studied with both cerium and silver as substrates. Figure 7(*a*) shows a plot of the relative attenuation of the Ag 3d emission with Ce deposition. The Ce evaporation rate was estimated to be (0.7 ± 0.1) Å min^{-1}. An attenuation less than the ideal exponential decay again indicates the formation of a non-homogeneous interface, supported by the measured shift in the Ag $3d_{5/2}$ core level (figure 2(*a*)) which indicates alloy formation. The peak shifts to higher binding energies, and the total shift slightly increases in size with increasing Ce layer thickness.

For the inverse system, Ag on Ce, the Ce substrate attenuation as a function of Ag evaporation time is plotted in figure 7(*b*), and the observed shifts to higher binding energies for the Ag $3d_{5/2}$ core level are plotted in figure 2(*b*). No tetravalent Ce photoemission was observed at any overlayer thickness for any of the Ce–Ag systems. This is consistent with the fact that all known Ce–Ag binary systems are trivalent.

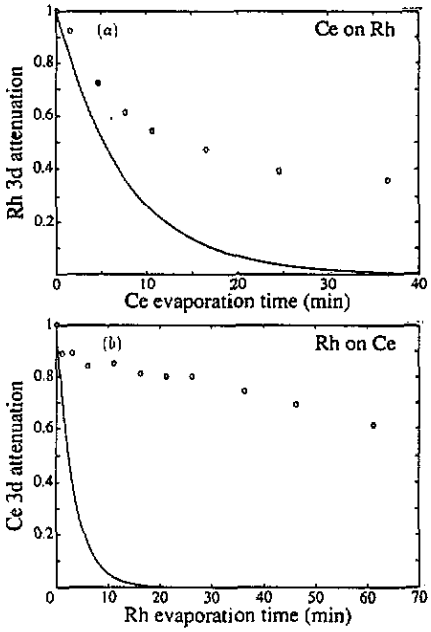

Figure 5. (*a*) Attenuation of Rh 3d photoemission with Ce deposition at a rate of ~ 2.2 Å min^{-1}. (*b*) Attenuation of Ce 3d emission with the deposition of a Rh overlayer at a rate of ~ 2.7 Å min^{-1}. The solid curve shows exponential attenuation.

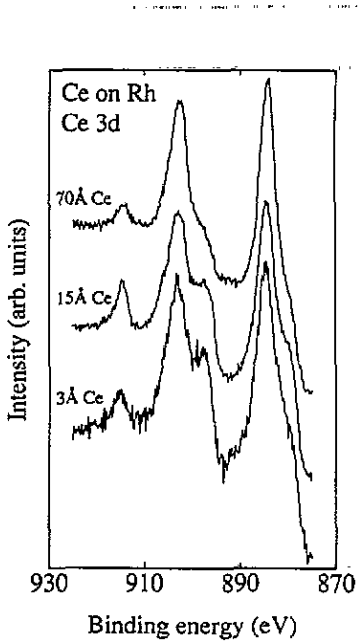

Figure 6. The Ce 3d core level spectra for a sample with Rh substrate and Ce overlayers of three different thicknesses: ~ 3 Å (lower curve), ~ 15 Å (middle curve) and ~ 70 Å (upper curve). Tetravalent Ce emission is observed in all three cases.

4. Discussion

As previously mentioned, different modes of overlayer growth may result in similar substrate core level attenuation curves. Even overlayer growth may be readily separated from clustering or reactive interface formation, but the latter two growth modes may be difficult to distinguish from each other on the basis of attenuation profiles. Our results show that substrate core levels are attenuated less, when material is deposited, than the ideal exponential decay which is expected from an even overlayer growth. This was observed in all the cases studied here, i.e. in the systems Ce on Rh, Pd or Ag, and in Rh, Pd, or Ag on Ce. Distinct shifts in the 4d metal substrate core levels show that a reaction is taking place in the interface. In addition, the observation of Ce $4f^0$ emission in the Ce–Rh and Ce–Pd systems shows that valence-unstable Ce alloys have been formed in the interface regions. However, it is not possible, on the basis of the present data, to rule out a possible tendency towards clustering of the deposited material on the surface, in addition to alloying. It seems that clustering may be less likely on evaporated substrates, which are polycrystalline or even amorphous in nature, as compared to being single-crystalline or preferentially oriented substrates.

The observation that Ce 3d peaks are attenuated at a slower rate when Rh is deposited onto a Ce substrate, as compared to that in the Pd on Ce system, which again shows slower attenuation as compared to the Ag on Ce system (see figures 1(*b*), 5(*b*) and 7(*b*)), is readily understood in terms of the fact that the surface free energy

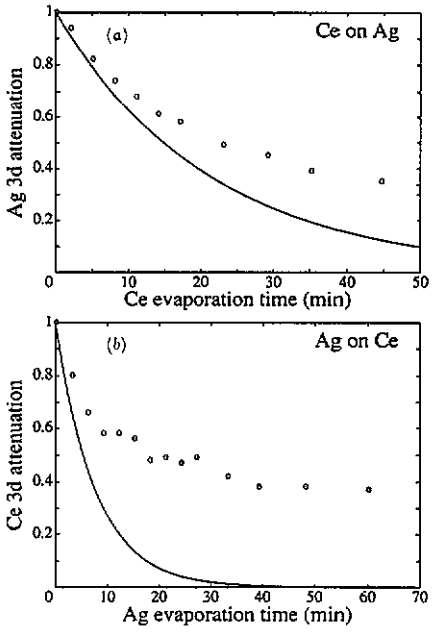

Figure 7. (*a*) Attenuation of the Ag 3d emission from the substrate as a Ce overlayer is evaporated at ~ 0.7 Å min^{-1}. (*b*) Ce 3d substrate attenuation as Ag is evaporated. The Ag evaporation rate was ~ 1.3 Å min^{-1}.

of Rh is larger than that of Pd, which in turn is larger than the surface energy of Ag [13]. It is therefore energetically favourable for Ce, which has a lower surface free energy, to be at the surface. The energy gain of having Ce at the surface is largest in the case of the Rh on Ce system, and hence explains the larger observed Ce content at the surface.

Several non-trivalent binary Ce–Rh and Ce–Pd intermetallic compounds exist, whereas all known binary Ce–Ag compounds are trivalent. The presence of a $4f^0$ signal in the Ce 3d emission in the Ce–Rh and Ce–Pd systems shows that the coordination around the Ce site is similar to that in mixed-valence compounds. However, the actual stoichiometric compounds probably do not form at room temperature. The $4f^0$ signal is seen to disappear in Ce-rich interfaces, which is in accordance with the fact that mixed-valence Ce–Rh and Ce–Pd compounds tend to have a transition metal content of more than 50%.

One might expect Ag to form alloys more readily than Pd, considering that Ag has a lower melting point and thus weaker interatomic bonds. The smaller core level shifts in the case of Ag are due to the fact that the size of a core level shift is not a measure of how easily a reaction takes place, but is rather a measure of the nature of the screening of the hole in the final state of the photoemission process. A shift to higher binding energies occurs when the screening is reduced. For the present systems this may be due to a reduction of electrons with 4d orbital symmetry in the 4d transition metals as Ag or Pd 4d orbitals overlap and hybridize with the Ce 4f electron orbitals in the ground state [14]. Differences in M 3d core level shifts in the Ce–M systems (M = Rh, Pd or Ag) may be qualitatively explained by differences in the electronic structure. Large shifts to higher binding energies for Pd

are indicative of a loss of the screening charge of 4d symmetry. Smaller shifts in Ag are consistent with the expectation that the completely filled Ag 4d band is less sensitive to stoichiometric changes. Shifts to lower binding energies in the Rh system indicate an increase in the screening charge of 4d symmetry, which is a result of hybridization between Rh and Ce states. The large differences in 3d core level shifts of the neighbouring elements Rh and Pd must be explained by considering details in the electronic structure of the Ce–Rh and Ce–Pd systems. Theoretical work seems to be needed to sort this out.

5. Summary

Mixed interface regions have been observed in Ce–Rh, Ce–Pd and Ce–Ag overlayer systems. Tetravalent Ce emission was observed in the Ce–Rh and Ce–Pd systems, whereas only trivalent emission was present in the Ce–Ag system. Substrate core level attenuation curves show a deviation from exponential decay as material is deposited. Substrate core level shifts and the appearance of a tetravalent Ce signal is indicative of interface alloy formation; however, clustering of the evaporated species may also take place. A large difference in 3d core level shifts in the Ce–Rh and Ce–Pd systems is observed. These shifts are due to a change in the density of electrons of 4d orbital symmetry in the initial state, which is caused by hybridization to Ce states. A complete understanding of the shifts calls for more theoretical work on the distribution of the screening charge in these systems.

References

[1] Lawrence J M, Riseborough P S and Parks R D 1981 *Rep. Prog. Phys.* **44** 1
[2] Mihalisin T, Scoboria P and Ward J A 1981 *Phys. Rev. Lett.* **46** 862
[3] Jayaraman A 1979 *Handbook on the Physics and Chemistry of Rare Earths* vol 2, ed K A Gschneidner Jr and L R Eyring (Amsterdam: North-Holland) p 575
[4] Parks R D, Raaen S, den Boer M L, Murgai V and Mihalisin T 1983 *Phys. Rev.* B **28** 3556
Raaen S and Parks R D 1985 *Phys. Rev.* B **32** 4261
[5] Schwarz R B and Johnson W L 1983 *Phys. Rev. Lett.* **51** 415
[6] Raaen S, Berg C and Braaten N A 1992 *Surf. Sci.* **269–70** 953
[7] Daniel M P 1979 *Handbook on the Physics and Chemistry of Rare Earths* vol 1, ed K A Gschneidner Jr and L R Eyring (Amsterdam: North-Holland) p 847
[8] Schmalzried H 1981 *Solid State Reactions (Monographs in Modern Chemistry 12)* (Weinheim: Chemie)
[9] Markov I and Stoyanov S 1987 *Contemp. Phys.* **28** 267
[10] Fuggle J C, Hillebrecht F U, Zołnierek Z, Lässer R, Freiburg Ch, Gunnarson O and Schönhammer K 1983 *Phys. Rev.* B **27** 7330
[11] Wertheim G K and Campagna M 1978 *Solid State Commun.* **26** 553
[12] Wuillod E, Delley B, Schneider W-D and Baer Y 1984 *Phys. Rev. Lett.* **53** 202
[13] Mezey L Z and Giber J 1982 *Japan. J. Appl. Phys.* **21** 1569
[14] Watson R E and Perlman M L 1975 *Struct. Bonding* **24** 83